Observation of the early stages of GaN thermal decomposition at 1200 °C under N2

H. Bouazizi, Mohamed Bouzidi, Noureddine Chaaben, Youssef El Gmili, Jean-Paul Salvestrini, A. Bchetnia

Observation of the early stages of GaN thermal decomposition at 1200 °C under N_2

H. Bouazizi[a], M. Bouzidi[a], N. Chaaben[a,*], Y. El Gmili[b], J.P. Salvestrini[b], A. Bchetnia[a]

[a] *Unité de Recherche sur les Hétéro-Epitaxies et Applications, Faculté des Sciences de Monastir 5019, Université de Monastir, Tunisia*
[b] *Unité Mixte Internationale, 2958 Georgia Institute of Technologie – Centre Nationale de la Recherche Scientifique, Université de Lorraine, 57070 Metz, France*

We investigated the partial decomposition of GaN layers grown in an atmospheric pressure metal organic vapor phase epitaxy (AP-MOVPE) vertical reactor at 1200 °C under N_2 ambient. In these conditions, the early stages of GaN thermal decomposition were studied. The GaN decomposition was monitored by in-situ laser reflectometry (LR). The properties of the as grown and decomposed GaN samples were analyzed by scanning electron mi-croscope (SEM). We show that GaN decomposition starts by the formation of GaN nano-grains at the early stages. Then, due to the anisotropy of the decomposition, the GaN nano-grains are more easily etched than the GaN (0 0 .2) surface. The lateral etching may results in local smooth GaN surface formation. After that the depth etching starts again on the etched pits. Room temperature cathodoluminescence (CL) study revealed better optical properties of the GaN grains when compared to the whole GaN surface.

1. Introduction

Due to their wide band gap and high thermal conductivity, III-nitrides materials have been employed for high-power and high temperature applications [1,2]. Among III nitrides group, gallium nitride (GaN) has received considerable attention because of its significant band gap value of 3.43 eV at 300 K. The structural, optical and electrical properties are critical for device performance and all these properties depend on the process temperature [3,4]. High temperature treatment of GaN is an essential processing part in device fabrication such as p-GaN doping (by Mg acceptors) activation and ohmic contacts realization for GaN based devices [5–10]. Thermal annealing process is also used to reduce the defects density in GaN [4,11]. Considerable improvements in surface morphology and PL intensity have been achieved by high temperature rapid thermal annealing of GaN [3]. The knowledge of the critical temperature, below which the GaN epitaxial layers remains stable under the high temperature annealing conditions, is of great interest. Most of the works on annealing of GaN showed that GaN properties are affected when the processing temperature exceeds 900 °C [5–7,11]. However, thermal treatments should be performed in thermodynamic conditions that avoid film decomposition. Several studies showed that the annealing of GaN at temperature beyond 1000 °C even in nitrogen causes decomposition in the near GaN surface region [12–14]. In previous works, we demonstrated that GaN decomposition starts from critical temperature beyond 700 °C under H_2 and 1100 °C under N_2 [15–17]. Bchetnia et al. [17] studied the annealing temperature on GaN decomposition rate in the range of 1000–1200 °C under N_2 environment in AP-MOVPE reactor. The GaN thermal decomposition has been studied by others groups versus several parameters that relates to decomposition environment such as temperature, pressure, carrier gas and geometry reactor [15–21]. However, little attention has been devoted to the effect of initial surface morphology on the partial GaN decomposition process. Recently, we investigated the relationships between the initial coalescence degree of GaN and its decomposition kinetic at 1200 °C under N_2 [22]. We demonstrated that decomposition of complete coalesced GaN can be performed nearly layer by layer and decomposition of incomplete coalesced GaN leads to anisotropy etching with high surface degradation [22]. The decomposed GaN layer until 0.6 μm of thickness loss showed crystalline property comparable to the as grown GaN layer. To the best of our knowledge, there is no work on the early stage of GaN thermal decomposition under N_2.

In this work, by using a coalesced GaN layer we investigated the different stages of GaN thermal decomposition at a fixed annealing temperature close to 1200 °C under N_2. We used the in situ time-reflectance and SEM to study the evolution of GaN surface state versus the early stages of its decomposition.

* Corresponding author.
E-mail address: noureddine.chaaben@fsm.rnu.tn (N. Chaaben).

2. Experimental details

The GaN layers were grown by AP-MOVPE on sapphire substrates at 1120 °C using the standard SiN treatment [23]. Trimethylgallium (TMGa), and ammonia (NH_3) were used as Ga, and N precursors, respectively. A mixture of H_2 and N_2 was used as carrier gas in MOVPE process. The heated reaction zone is obtained through induction heating and the backside temperature is monitored by S-type thermocouple and feedback system. The standard growth experiments start with the sapphire substrate nitridation under NH_3 at 1080 °C for 10 min. Then, the SiN treatment is carried out at the same temperature during 75 s under NH_3 and silane (SiH_4) flows. Then, the temperature is decreased down to 600 °C to grow nominal 30 nm thick GaN buffer layer. Afterwards, the temperature is increased to 1120 °C to grow the GaN sublayer. Firstly, the GaN growth starts by three-dimensional (3D) mode with a large surface roughness. Due to a coalescence process the GaN layer progressively undergoes a transition from 3D to 2D growth mode that finally leads to smooth surface. The as grown GaN sample is referenced as A_0. Four cut up GaN samples were annealed at 1200 °C in AP-MOVPE reactor under pure N_2 (2 slm). After their partial decomposition the samples are labeled A_1, A_2, A_3 and A_4. The annealing treatment of each sample was stopped at different stages corresponding to thickness loss in the range of 0–0.6 μm. The growth and decomposition processes were in situ controlled by He-Ne-laser reflectometry ($\lambda = 632.8$ nm) at normal incidence light. The surfaces of the annealed samples were ex-situ examined by SEM and CL at room temperature using 3 keV electrons beam.

3. Results and discussion

Fig. 1 shows a typical record of the in situ laser reflectivity signal obtained during growth (steps a–c) and decomposition (step d) of GaN. The reflectivity signal during growth and decomposition is normalized with respect to the last and first maxima, respectively. During the temperature ramp to 1200 °C, we found that when the temperature reach a 1100 °C value, as indicated by the arrow 2 in Fig. 1, the reflectivity signal shows an abrupt increase before it start to oscillate. This behavior occurred for all GaN decomposition experiments in the same conditions. This can indicate firstly a critical temperature of GaN decomposition under N_2 about 1100 °C and secondly a high reflective GaN

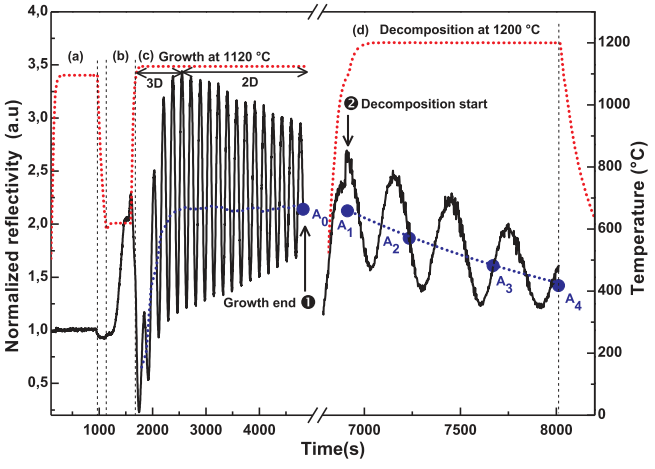

Fig. 1. In situ laser reflectivity measurements during growth and partial decomposition of GaN. The growth steps shown in this figure are: (a) nitridation during 10 min followed by short time (75 s) SiN treatment of sapphire substrate at 1100 °C, (b) low temperature (600 °C) GaN buffer layer growth, (c) temperature ramp from 600 °C to 1120 °C, (d) growth of high temperature (1120 °C) GaN sub-layer starting by 3D growth mode and followed by 3D-2D transient mode until complete coalescence. The step (d) corresponds to GaN decomposition at 1200 °C under pure N_2. The arrows 1 and 2 indicate growth end and decomposition start, respectively. The points labelled (A_1–A_4) indicate the stage at which the decomposition was interrupted.

surface due to formation of Ga rich GaN surface originating in a preferential evaporation of N_2 [24]. When the temperature reaches a constant value of 1200 °C, the GaN decomposition takes place and the reflectivity signal oscillations indicate a GaN thickness loss. From the oscillation period (T) of in situ time-reflectance ($R(t)$), the growth rate and decomposition rate (V) were calculated by using the following equation: $V = \frac{\lambda}{2nT}$ (Eq. (1)). Where n is the refractive index for the used wavelength. Then the layer thickness (d) can be calculated from the equation: $d = V.\,\Delta t$ (Eq. (2)). Where, Δt is the duration of process. For the buffer layer thickness control, we used the ratio ($r = \frac{R_b}{R_s}$) (Eq. (3)) of buffer layer reflectance (R_b) by the substrate one (R_s). For the growth of sample A_0, we measured these growth rate values 0.34 μm/h and 2.77 μm/h for GaN buffer layer and GaN sublayer, respectively. The as grown GaN sublayer presents a total thickness close to 2.48 μm, where 0.73 μm is reached in 3D growth step and 1.75 μm is reached in 2D growth step. From the in situ time-reflectance recorded during the decomposition process, if we have several oscillation periods, by using Eq. (1) and Eq. (2) we can calculate an average value of decomposition rate. In case of sample A_4, the calculus gives an average decomposition rate close to 1.61 μm/h. In case of lower thickness loss such as stages A_2 and A_3, for which the oscillations numbers are insufficients, the ex-situ multi wave reflectance ($R(\lambda)$) technic gives more accurate measurements of decomposed GaN thickness. The measurements of thickness are detailed in Table 1 and Table 2. In these experiments, because the maximum thickness loss is 0.60 μm, we will discuss about partial decomposition of 2D GaN layer.

Fig. 2 shows the multi-wave reflectance spectra for samples A_0–A_4 measured in wavelength range of 200–1100 nm at normal incidence. The reflectance spectra show that for wavelengths higher than the corresponding GaN gap (365 nm), the GaN film is transparent and multiple optical interferences take place within the epitaxial layer. This explains the observed reflectance oscillations with a magnitude and period that are related to thickness and optical constants (n and k) film. Smooth and flat GaN surface and GaN/substrate interface give very pronounced oscillations. From spectra in Fig. 2, the film thickness (d) can be calculated in each period by the following equation [25]:

$$d = \frac{\lambda_1\lambda_2}{2(\lambda_1 n_2 - \lambda_2 n_1)} \qquad \text{(Eq. (4))}$$

where λ_1 and λ_2 are the wavelengths for two adjacent same type of extreme (max or min) and n_1 and n_2 are their corresponding refractive index values. The variation of GaN refractive index versus wavelength was taken from Ref. [26]. By summing over all periods of pronounced oscillations an average ($\bar{d}$) was calculated and taken as the film thickness. In Table 1 we give as example the sample A_4 thickness calculus using this method. The thickness loss ($d_l = d_i - \bar{d}$) (Eq. (5)) is given by the difference between the thickness of the as grown GaN layer (d_i) and the average decomposed thickness ($\bar{d}$). Table 2 gives the surface roughness values (derived from average reflectivity) of samples A_0–A_1 as well as their corresponding thickness values calculated using time-reflectance and multi-waves reflectance spectra. The values of thickness given by the two methods are in good agreement. The sample A_1 was annealed until 1100 °C, so its thickness remains close to that of sample A_0.

Fig. 3 shows the SEM images of the top surface of sample A_2, where it can be seen some flower-like particles, with an average size of around 5 μm, surrounded by a high density of GaN nano-grains. The flower-like particles (with the same size) are present in other decomposition stages.

Fig. 4 shows high magnification SEM images corresponding to the as grown GaN (A_0) and the region between GaN nano grains for the decomposed samples (A_1–A_4). For the as grown sample we observed a smooth and flat GaN surface which is in good agreement with the high reflectivity contrast corresponding to a coalesced GaN layer. The SEM image of sample A_1 shows homogenous structure formed by nano-grains. The presence of nano-grains could indicate the beginning of GaN

Table 1
Details of film thickness calculus with error from max and min pairs of multi-wavelength reflectance of sample A_4.

Order m	Extremes-type	λ_1 (nm)	λ_2 (nm)	n_1	n_2	d (μm)	$\bar{d}$ (μm)	Erreur	$\overline{\text{Erreur}}$
1	Max	634	681	2.385	2.375	1.98	**1.91**	0.078	**0.06**
2	Max	681	737	2.375	2.366	1.90		0.066	
3	Max	737	804	2.366	2.358	1.90		0.056	
4	Max	804	884	2.358	2.352	1.93		0.049	
1	Min	613	657	2.391	2.380	1.89		0.082	
2	Min	657	708	2.380	2.371	1.92		0.073	
3	Min	708	768	2.371	2.362	1.92		0.063	
4	Min	768	843	2.362	2.355	1.87		0.050	

Table 2
Thickness and surface roughness values of the as grown and decomposed GaN samples A_0–A_4. The surface roughness (σ) and thickness (d) values were estimated from in situ time-reflectance ($R(t)$) of Fig. 1. We considered as average value V_d = 1.61 μm/h of the GaN decomposition rate. For comparison, we give the thickness ($\bar{d}$) values deduced from ex-situ multi-wave reflectance spectra ($R(\lambda)$).

Sample	A_0	A_1	A_2	A_3	A_4
Thickness from $R(t)$:					
$d = V_d.\ \Delta t$ (μm)	2.48	2.45	2.28	2.09	1.94
Thickness from $R(\lambda)$:					
$\bar{d}$ (μm)	2.51 ± 0.09	2.50 ± 0.08	2.32 ± 0.10	2.12 ± 0.10	1.91 ± 0.06
Thickness loss:					
$d_l = (d_i - \bar{d})$ (μm)	0	0	0.18	0.38	0.60
σ (nm)	22	22	25	30	38

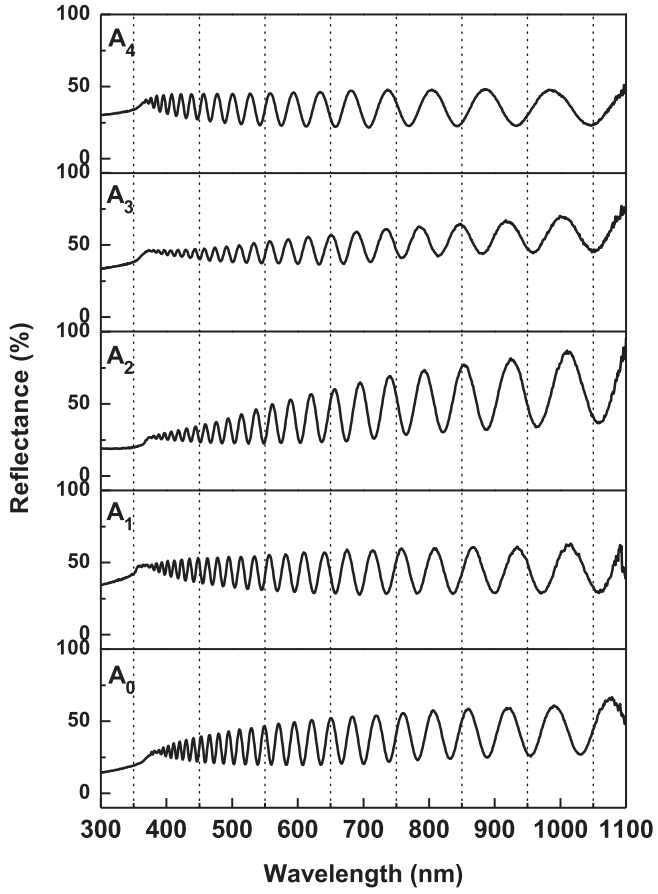

Fig. 2. UV–Visible normalized reflectance spectra corresponding to the as grown A0 and partially decomposed A_1–A_4 samples. The multi-wave reflectance data's are normalized using the formula: $R_{normalized} = 100\frac{(R_{sample} - R_{dark})}{(R_{reference} - R_{dark})}$. Where R_{sample} and $R_{reference}$ are the reflectances of sample and substrate, respectively and R_{dark} is measured when the incident light source is turned off.

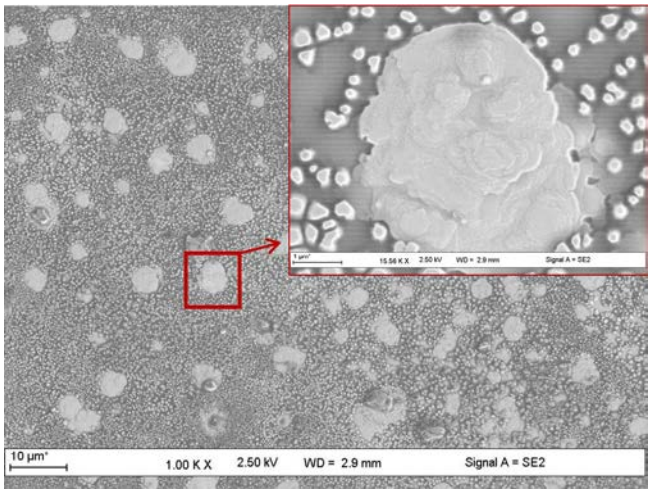

Fig. 3. Scanning electron microscopy (SEM) image of annealed GaN at stage A_2. The scale bars of insets images are 1 μm to show more details for flower-like particle.

decomposition. It is known that the thermal decomposition preferentially starts on dislocations sites which are normally more generated near the interface region [27]. However, at the second stage (A_2) corresponding to a decomposition of 165 nm-thick GaN, we observed hexagonal shape GaN nano-grains with relatively large size exceeding 400 nm. The hexagonal GaN hillocks are truncated and the spacing between them shows a flat and smooth surface. Surprisingly, the grain structure was not observed at the third stage (A_3) corresponding to a decomposition of 360 nm-thick GaN. The sample A_3 shows a smooth and flat surface with presence of etch pits whose density was approximatively $D_e = 1.5{\cdot}10^8\ cm^{-2}$. This value is of the same order of magnitude as the initial dislocation density $D_d = 6.1{\cdot}10^8\ cm^{-2}$ of the as grown sample. After decomposition of 500 nm-thick GaN (stage A_4) we observed a flat GaN surface with presence of some hexagonal shape GaN hillocks and some others generated hexagonal facets. From these morphological observations we can suggest that there are two decomposition processes. The first one deals with vertical decomposition rate which leads to grains structures. This first process can be limited when

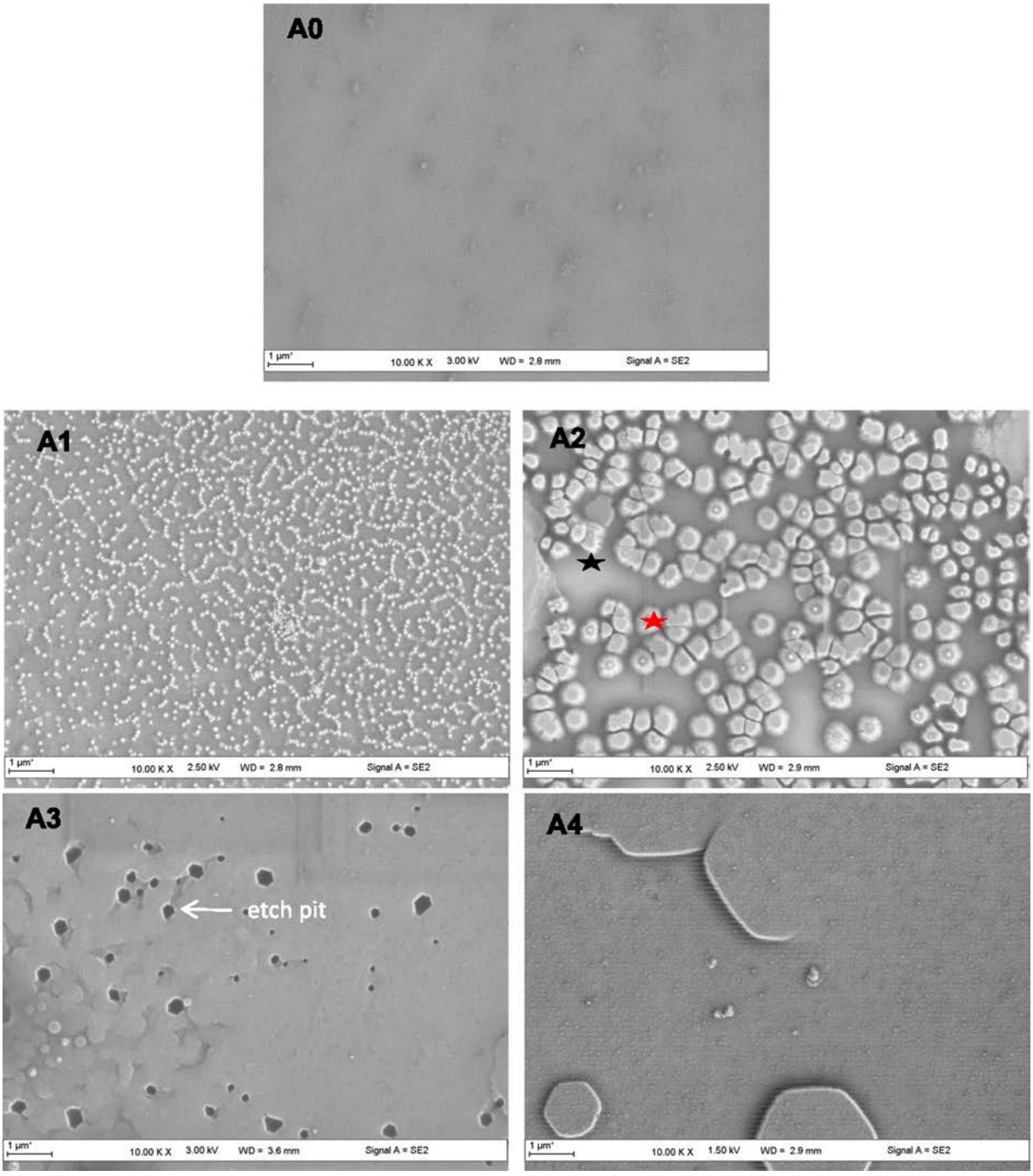

Fig. 4. Scanning electron microscopy (SEM) images of as-grown GaN (a) and annealed GaN surfaces (b) A_1, (c) A_2, (d) A_3 and (e) A_4. The scale bar corresponds to 1 µm.

large surface of hexagonal facets are generated. The second process takes place with lateral decomposition rate until complete decomposition of GaN hillocks (case of sample A_3), except of the flower-like particles as described in Fig. 3 that showed etching resistance.

The presence of isolated GaN grains in samples A_1 and A_2 indicated that vertical process has already taken place and lateral process is in progress. Because of the GaN grains size is bigger in sample A_2 compared to sample A_1, it seems that the stages A_1 and A_2 correspond to two different vertical-lateral decomposition cycles. The first lateral process (via stage A_1), which leads to free surface grain, is followed by a new vertical process and then a second lateral process is occurred (via stage A_2).

Lateral and vertical decomposition processes indicate an anisotropy of GaN decomposition that can be associated with the thermal stability differences between the in plane c(0 0 .1) and out of plane facets. The vertical-lateral decomposition cycle can take place if the GaN surface degradation is still very low. But for the advanced GaN decomposition stage, the high surface roughness leads to an irregular etching. In that condition the locally smooth surface like in case of samples A_3 and A_4 could not be observed. Furthermore, the GaN decomposition can be achieved in its last stage by a porous structure and gallium droplet formation [17]. In this experiment, we observed just the early stages until decomposition of about 600 nm-thick GaN. There are several mechanisms that have been proposed to explain how GaN decomposes into liquid GaN ($2GaN(s) \rightarrow 2Ga(l) + N_2(g)$) and into gaseous Ga and N ($2GaN(s) \rightarrow 2Ga(g) + N_2(g)$) and/or sublimation of GaN ($GaN(s) \rightarrow GaN(g)$) [13,20]. However, because of the absence of Ga droplets until decomposition of 500 nm of GaN, we can propose that at

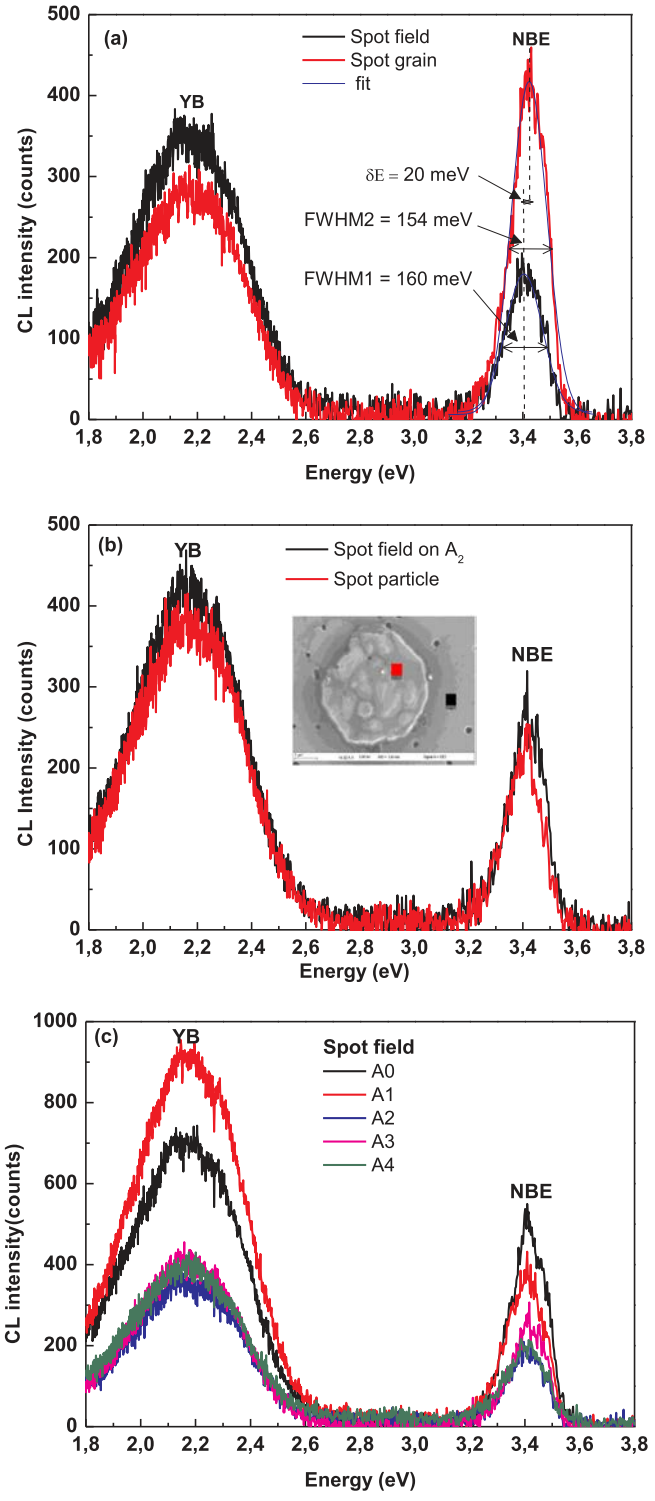

Fig. 5. The CL spectra down at room temperature with 3 keV electrons beam (a) on and out of GaN grains region as mentioned by stars in micrograph of Fig. 4 corresponding to sample A_2, (b) on and out of flower-like particle as mentioned by squares in the insert micrograph corresponding to sample A_2 and (c) on the field of A_0–A_4 samples.

the early stages the GaN decomposition proceeds by the two latter mentioned reactions.

For samples A_0–A_4, the surface roughness increases from 22 nm to 38 nm. These values were estimated from reflectivity signal. However, despite the surface smoothing at decomposition stage of A_3, the reflectivity signal still decreases. The monotonic decrease of the reflectivity signal even for smoothing cycles can be explained by the presence of the flower-like particles with micrometric size (see Fig. 3) which led in all cases to the reflectivity signal scattering.

Fig. 5a shows a set of CL spectra recorded with an acceleration voltage of 3 kV for two regions as assigned in Fig. 3 (spot grain and spot field). Each spectrum presents two peaks at 3.40–3.42 eV and 2.19 eV, respectively. The peak appearing at 2.19 eV is most likely related to GaN yellow band (YB). For the GaN surface, the peak located at 3.40 eV corresponding to the GaN near band edge (NBE) emission is slightly red shifted by 20 meV from the NBE of bulk unstrained GaN (3.42 eV) [28]. This red shift indicates a slight tensile strain in the GaN layer which is increased after partial decomposition by comparison with the NBE of the as grown GaN (3.41 eV). In contrary, the NBE related peak is located at 3.42 eV for the GaN micro-grains indicating a complete relaxed strain. The small dimensions of the isolated GaN micro-grains allows for local strain relaxation permitting the in plane lattice parameter to approach its bulk value [29,30]. By comparing the intensities and the FWHM of the two NBE emission peaks, we can conclude that the optical quality of the GaN micro-gains is higher and can be attributed to its lower dislocation density. The dislocation density reduction in the micro-grains is associated with the preferential decomposition start on dislocations sites. This result shows how thermal decomposition of GaN can be used to reduce strain and defect in GaN columns. The CL spectra, locally done on and out of flower-like particles (see Fig. 5b) showed similar spectra corresponding to GaN band edge emission. These comparable optical properties indicate an etching resistance in some zones which stops the decomposition process and allows to the flower-like particles formation. The CL spectra presented in Fig. 5c showed that the CL intensity of NBE emission peak decreases versus thickness loss indicating low optical quality in the field (out of grains and particles) for the advanced decomposition stage. This degradation of the optical quality can be related to the surface defects revelation (etch pits, roughness) due to decomposition process.

4. Conclusion

We studied the early stages of thermal decomposition of coalesced GaN layers under N_2 ambient at 1200 °C in MOVPE reactor operating at atmospheric pressure. SEM analyses of surface morphology evolution versus thermal decomposition stage images showed formation of GaN nano-grains. We have highlighted lateral and vertical decomposition processes at the early stages, due to anisotropy of decomposition. CL analyses showed unstrained GaN grains with higher optical quality. We suggest that thermal decomposition can be used to simply achieve GaN nanostructures with high optical qualities. Further investigations on the control of decomposition duration will be conducted.

References

[1] S. Nakamura, Frasol, The Blue Laser Diode, Springer, Berlin, 1999.
[2] H. Morkoc, S. Strite, G.B. Gao, M.E. Lin, B. Sverdlov, M. Burns, J. Appl. Phys. 76 (1994) 1363.
[3] J.C. Zolper, M. Hagerott Crawford, A.J. Howard, Appl. Phys. Lett. 68 (1996) 200.
[4] H. Siegle, G. Kaczmarczyk, L. Filippidis, A.P. Litvinchuk, A. Hoffmann, C. Thomsen, Phys. Rev. B 55 (1997) 7000.
[5] S. Nakamura, T. Mukai, M. Senoh, N. Iwasa, Jpn. J. Appl. Phys. 31 (1992) L139.
[6] H. Amano, M. Kito, K. Hiramatsu, I. Akasaki, Jpn. J. Appl. Phys. 28 (1989) L2112.
[7] M.A. Khan, Q. Chen, R.A. Skogman, J.N. Kuznia, Appl. Phys. Lett. 66 (1995) 2040.
[8] J. Hejtmánek, K. Knížek, M. Maryško, Z. Jirák, D. Sedmidubský, Z. Sofer, V. Peřina, H. Hardtdegen, C. Buchal, J. Appl. Phys. 103 (2008) 07D107.
[9] Y.S. Cho, H. Hardtdegen, N. Kaluza, N. Thillosen, R. Steins, Z. Sofer, H. Lüth, Phys. Status Solidi C 3 (6) (2006) 1408.
[10] Z. Sofer, D. Sedmidubský, M. Moram, A. Macková, M. Maryško, J. Hejtmánek, C. Buchal, H. Hardtdegen, M. Václavů, V. Peřina, R. Groetzschel, M. Mikulics, Thin Solid Films 519 (2011) 6120.
[11] J. Hong, J.W. Lee, J.D. MacKenzie, S.M. Donovan, C.R. Abernathy, S.J. Pearton, J.C. Zolper, Semicond. Sci. Technol. 12 (1997) 1310.
[12] M. Senthil Kumar, G. Sonia, V. Ramakrishnan, R. Dhanasekaran, J. Kumar, Physica B 324 (2002) 223.
[13] M.A. Rana, T. Osipowicz, H.W. Choi, M.B.H. Breese, F. Watt, S. Chua, J. Appl. Phys. A 77 (2003) 103.
[14] H.W. Choi, M.A. Rana, S.J. Chua, T. Osipowicz, J.S. Pan, Semicond. Sci. Technol. 17

(2002) 1223.
[15] A. Rebey, T. Boufaden, B. El Jani, J. Cryst. Growth 203 (1999) 12.
[16] W. Fathallah, T. Boufaden, B. El Jani, Phys. Status Solidi C 4 (2007) 145.
[17] A. Bchetnia, I. Kemis, A. Touré, W. Fathallah, T. Boufaden, B. El Jani, Semicond. Sci. Technol. 23 (2008) 125025.
[18] M. Kuball, F. Demangeot, J. Frandon, M.A. Renucci, J. Massies, N. Grandjean, R.L. Aulombard, O. Briot, Appl. Phys. Lett. 73 (1998) 960.
[19] D.D. Koleske, M.E. Coltrin, M.J. Russell, J. Cryst. Growth 279 (2005) 37.
[20] D.D. Koleske, A.E. Wickenden, R.L. Henry, J.C. Culbertson, M.E. Twigg, J. Cryst. Growth 223 (2001) 466.
[21] M.A. Mastro, O.M. Kryliouk, M.D. Reed, T.J. Anderson, A. Davydovand, A. Shapiro, Phys. Status Solidi A 188 (2001) 467.
[22] H. Bouazizi, N. Chaaben, Y. El Gmili, A. Bchetnia, J.P. Salvestrini, B. El Jani, J. Cryst. Growth 434 (2016) 72.
[23] A. Bchetnia, A. Touré, T.A. Lafford, Z. Benzarti, I. Halidou, M.M. Habchi, B. El Jani, J. Cryst. Growth 308 (2007) 283.
[24] S.J. Pearton, J.C. Zolper, R.J. Shul, F. Ren, J. Appl. Phys. 86 (1999) 1.
[25] S. Condurache-Bota, N. Tigau, R. Drasovean, J. Sci. Arts 13 (2010) 335.
[26] U. Tisch, B. Meyler, O. Katz, E. Finkman, J. Salzman, J. Appl. Phys. 89 (2001) 2676.
[27] N. Faleev, H. Temkin, I. Ahmad, M. Holtz, Yu. Melnik, J. Appl. Phys. 98 (2005) 123508.
[28] S.W. Lee, J.-S. Ha, H.-J. Lee, H. Goto, Appl. Phys. Lett. 94 (2009) 082105.
[29] E. Calleja, M.A. Sánchez-García, F.J. Sánchez, F. Calle, F.B. Naranjo, E. Muñoz, U. Jahn, K. Ploog, Phys. Rev. B 62 (2000) 16826.
[30] L. Cerutti, J. Ristić, S. Fernández-Garrido, E. Calleja, A. Trampert, K.H. Ploog, S. Lazic, J.M. Calleja, Appl. Phys. Lett. 88 (2006) 213114.